Supporting Information

The Effect of Water on the Validity of Löwenstein's Rule

Christopher J. Heard,*[a] Lukáš Grajciar[a] and Petr Nachtigall[a]

Contents

I: Single Water Loading

The two important adsorption modes for a single water molecule are denoted BAS: adsorption to the Brønsted acid site through an O-down interaction between water and a localized Brønsted proton, and anti-BAS: O-down interaction between water and the aluminium atom, in an anti-position to the Brønsted acid group. These modes are shown schematically in figure S1. The four inequivalent oxygen atoms surrounding the aluminium in CHA lead to four distinct BAS and anti-BAS adsorption sites. Adsorption to the proton at the BAS is found to be significantly preferred for all BAS sites in our simulations at 300 K, and so we do not consider the anti-BAS adsorption mode further here. An overall preference for adsorption was found at the O4 site.

The effect of water adsorption on the framework structure is probed with average bond lengths for the various adsorption sites. The presence of water at BAS sites slightly shortens the Al-O_f bond length from its bare H-CHA value of 1.91 Å (1.92 Å at 370 K), partially weakening the bond, but the effect is moderate.
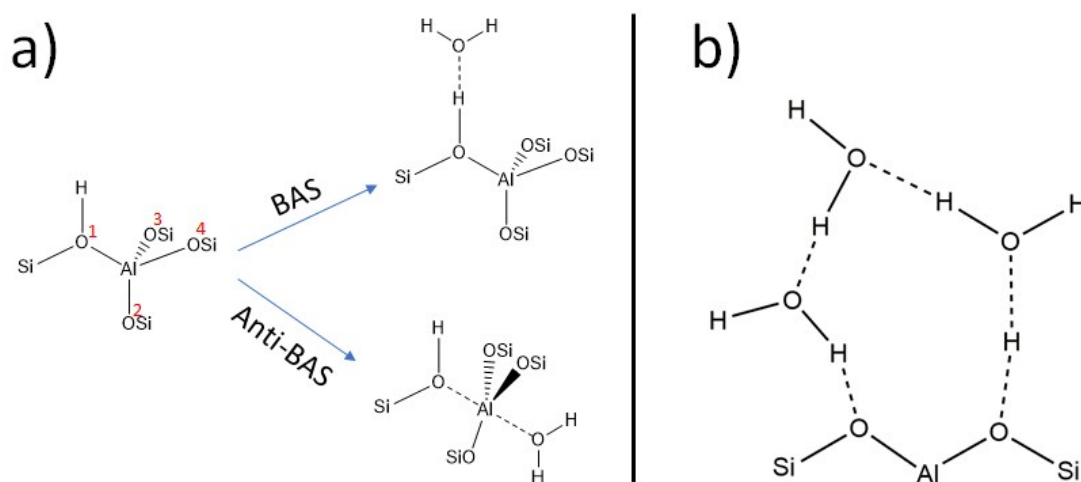
Figure S1: Comparison of water adsorption modes to the framework. a) - In the presence of a single water, water may bind in BAS or anti-BAS arrangements. b) – Water deprotonates the Brønsted site under full solvation, leading to a charge separated structure.

| Adsorption site	Relative Energy (kJ/mol)	Average Al-O_f bond length (A)	Average O_f-H bond length (A)	Average H-O_w bond length (A)
O(1)H (BAS)	+12 (+19)	1.87 (1.88)	1.16 (1.12)	1.33 (1.41)
O(2)H (BAS)	+14 (+20)	1.88 (1.88)	1.08 (1.07)	1.47 (1.52)
O(3)H (BAS)	+7 (+8)	1.85 (1.85)	1.07 (1.07)	1.47 (1.49)
O(4)H (BAS)	0 (0)	1.87 (1.87)	1.09 (1.10)	1.43 (1.43)

Table S1: Average relative internal energies and bond lengths for low water loading conditions from *Ab Initio* MD simulations at 300 (370) K.
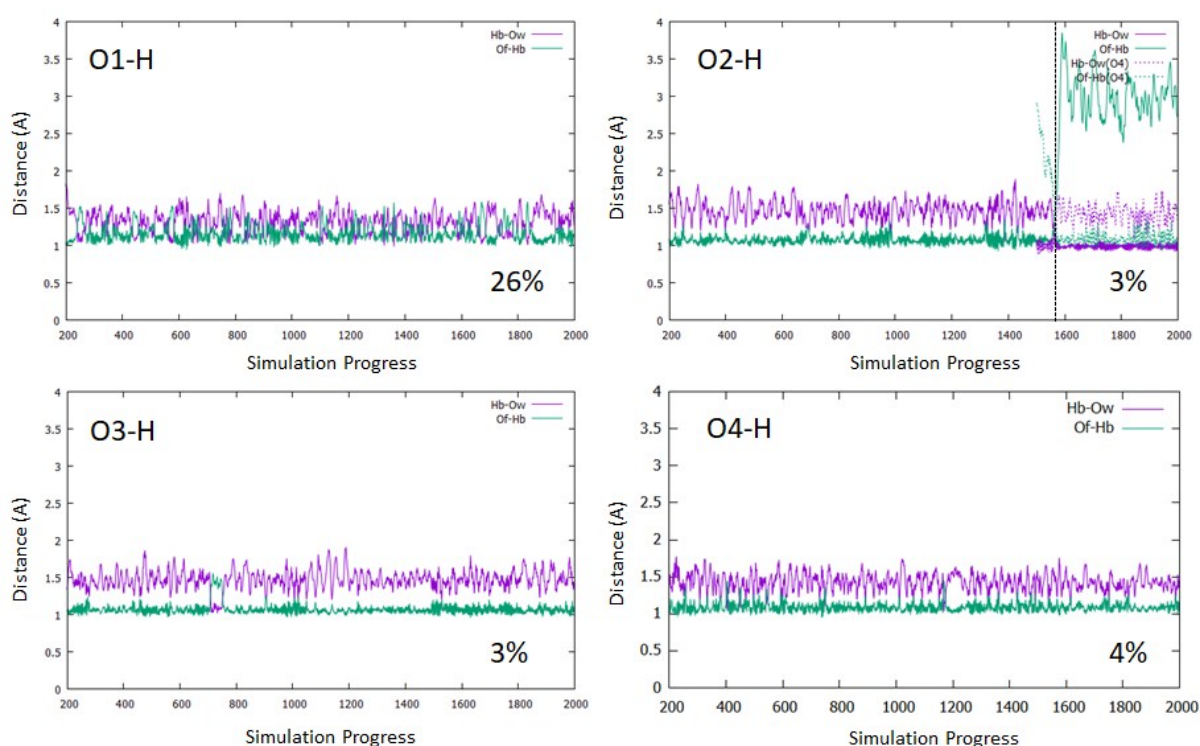
Figure S2: Traces of the O_f-H_b and H_b-O_w bond distances for the O1, O2 , O3 and O4 BAS sites at 300 K under low water loading conditions. Percentage degree of solvation (H^+ being closer to O_w than to O_f oxygen atoms) is given in insets.

Under low water loading, the water molecule adsorbs to the BAS. The O4 site is the most stable adsorption site, as shown in table S1. O1 shows the highest degree of solvation (26 %) owing to the shape of the site. The H_3O^+ group is stabilised in a symmetrical position above the face of the 6-ring. It can form H-bonds to three framework oxygens at once, and so has a significant proportion of solvated states. O2, O3 and O4 all show a significantly smaller degree of solvation (3, 3 and 4 %), respectively. The O2 site undergoes an exchange, with H_3O^+ hopping from O2 to the nearby O4 site after around 8 ps of simulation time, due to the greater stabilisation of water on O4, and the short distance between the two sites. A related

coupled proton hopping event is described between this pair of O_f sites under full water loading conditions in the main article. The proton does not remain solvated, as seen in the distance trace. The H_3O^+ instantaneously binds to the O4 site through another H_w, forming a new, strongly bonded BAS.
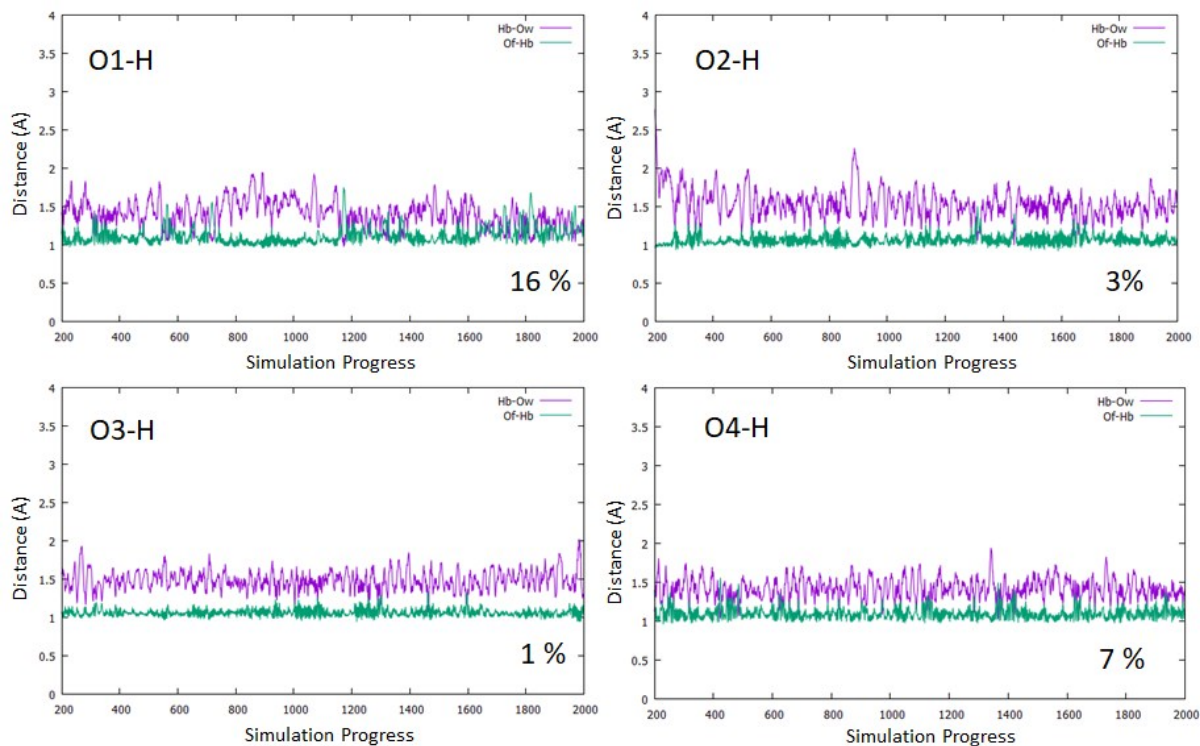
Figure S3: Traces of the O_f-H_b and H_b-O_w bond distances for the O1, O2 , O3 and O4 BAS sites at 370 K under low water loading conditions.

The role of temperature in the range 300-370 K is found to be small. The degree of solvation of the O1 site is reduced. However, the effects on the other O_f sites is not significant.

II: High Water Loading (370 K)
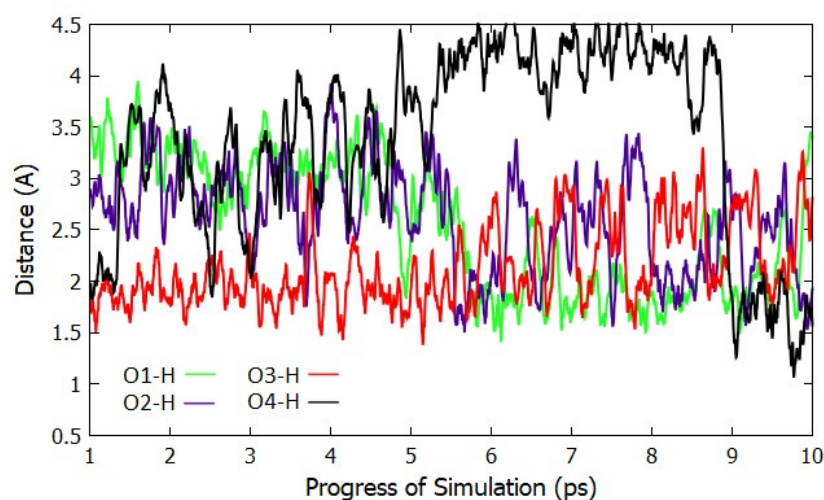
Figure S4: Trace of the minimum O_f-H distances for high water loading at 370K (Si:Al = 11). There are coupled proton hops between O1 and O3, in accordance with the simulation at 300 K. The minimum distances span a similar range as at 300 K, with 13 % (10 % at 300 K) of configurations showing a minimal distance below 1.5 A, and 31 % (19 % at 300K) with a minimal distance above 1.9 A. The degree of solvation is > 99 %, in accordance with the findings at 300 K.

III: Pair Distribution Functions
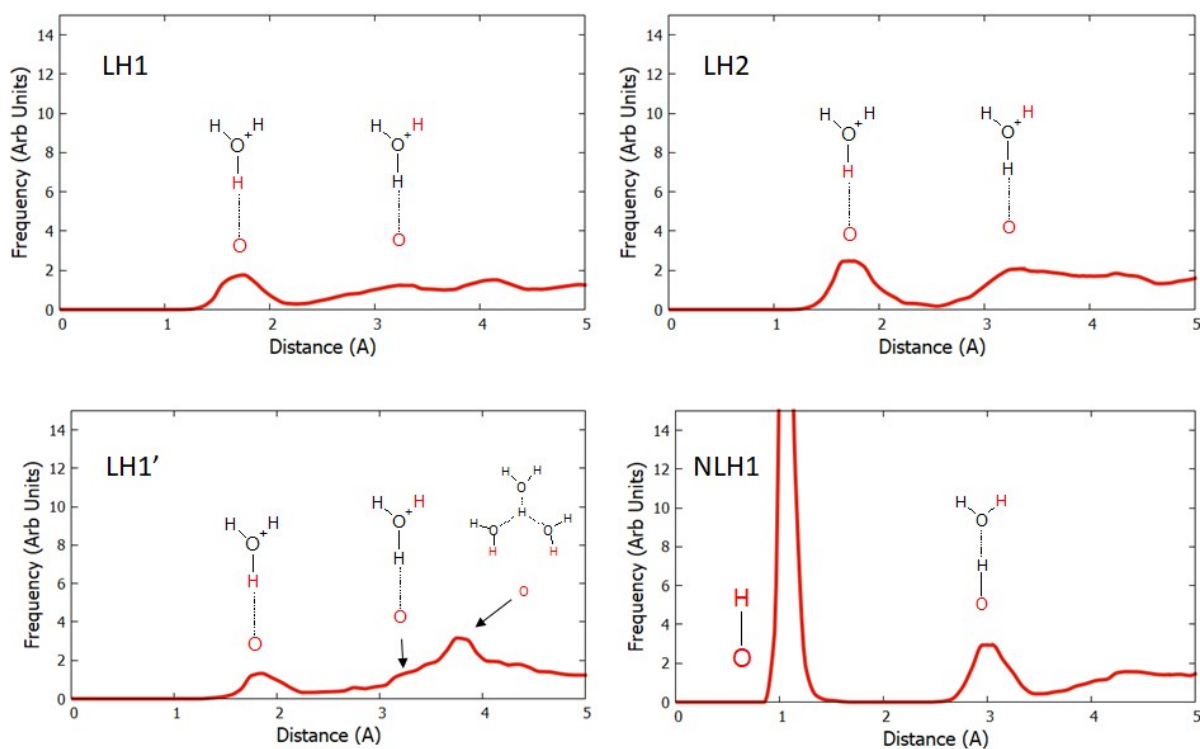
Figure S5: Comparison between the PDFs of LH1, LH1, LH1' and NLH1 O-H distances. LH1 and LH2 are similar, as these are formally identical sites. LH1', which is the most acidic of all four considered sites, is qualitatively similar to LH1/LH2, with peaks due to the two O_f-H-OH_2^+ distances, at 1.8 and 3.2 Å. LH1' also shows a peak at 3.9 Å due to the distance from the nearest H_w of a protonated cluster in the free pore volume.

IV: Visualization of Simulations

Animations are attached (in .gif format) to highlight important features of several of the simulations.

a) 300K-high-water.gif: Visualisation of one of the cages of H-CHA (Si:Al=11) at 300 K under high water loading conditions. The animation shows that there is a protonated water cluster, which forms transient hydrogen bonds to the O1 and O3 framework sites. Thus, the charge separated regime described in the main article is maintained, rather than de-solvation of H_b and regeneration of the H_b-O_f bond.

b) NLH1.gif: Visualisation of the cage connected to the NLH1 site in the non-Löwenstein isomer (Si:Al=17). The animation shows that there is a water molecule bound to the Brønsted proton of the Al-O(H)-Al moiety which forms a neutral water cluster in the pore. The O_f-H_b bond remains throughout the simulation due to its low acidity.

V: H-ABW

In order to generalise the results of H-CHA, we have considered the energetic and solvation properties of the dense zeolite H-ABW, which contains independent one-dimensional channels. The accessible pore volume is 5.19 % (c.f. 17.27 % in CHA) [1] with a maximum probe sphere diameter of 4.24 Å (c.f. 7.27 Å in CHA)[1] within the microporous channel. The model chosen was a 2x1x1 supercell, containing two aluminium sites (and two Brønsted acid protons) per supercell, with an Si:Al ratio of 7. The cell parameters were 9.87 Å x 10.51 Å x 8.77 Å. Configurations were chosen to contain Brønsted acid sites which are exposed to different channels, in order to avoid inhomogeneity in the H_2O:H^+ ratio across different pores.

DFT+D3 (BJ) incorporation energies (E_{inc}) of "n" successive water molecules into the channel were determined in the athermal regime, via local geometry optimisation, according to the equation:

$$E_{inc} = E_{ABW+n.H2O} - E_{ABW} - n.E_{H2O(gp)}$$

For n = 1, 2 and 3, E_{inc} was calculated to be -1.1, -1.7 and -2.4 eV, respectively. Hence, higher water loadings than 1 H_2O/Brønsted acid site in the channel are predicted to be realistic.
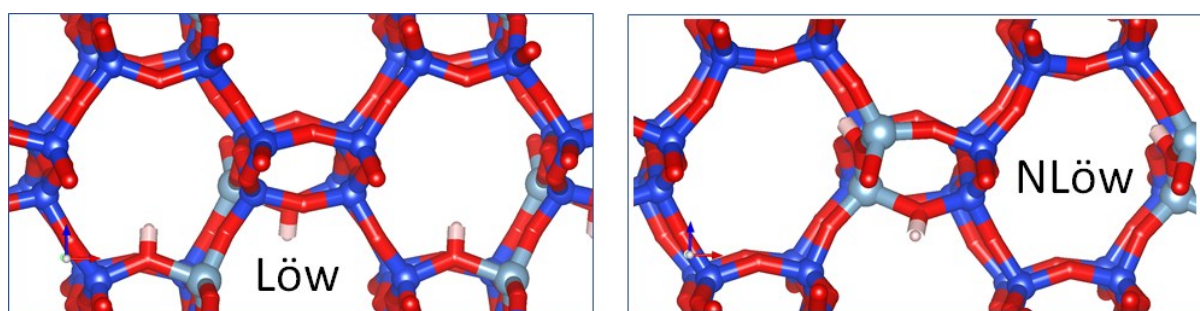

Figure S6: Structural models of the Löw and NLöw configurations considered in H-ABW. Channels are perpendicular to the projection. Si: dark blue, Al: light blue, O: red, H: white.

Under anhydrous, athermal conditions, the chosen NLöw configuration is found to be 0.01 eV more stable than the Löw configuration.

To determine the role of water on the energetic and solvation properties of H-ABW, equilibration AIMD simulations were run for 20 ps at 300 K for both configurations, with three water molecules included per channel. In correspondence with H-CHA, we observe that both protons are quickly solvated (< 2 ps) and remain solvated for the duration of the simulation for the Löw configuration. The same behaviour is observed for the Al-O(H)-Si proton in the NLöw configuration. The Al-O(H)-Al proton is not found to be solvated for the duration of simulation, in accordance with the findings for H-CHA. The relative average internal energy of NLöw is +0.40 eV with respect to Löw at 300 K (Fig. S7). Hence, both qualitatively, and quantitatively the same behaviour is observed for H-ABW as for

H-CHA, which suggests that the topological effects are not significant, given a comparable level of water loading.
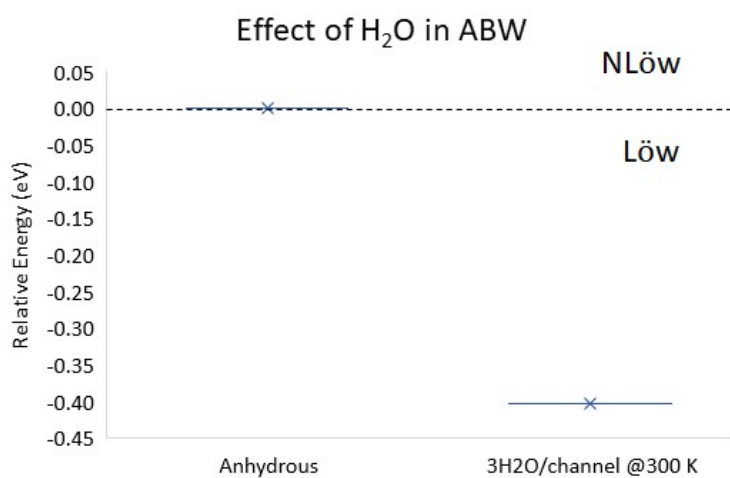
Figure S7: Comparison between athermal, anhydrous relative energies and AIMD relative energies under solvation, for the pair of configurations in H-ABW.

References:

1: IZA database. http://www.iza-structure.org/databases/, 2017